Volume 14, Issue 3, 142432 (1-15)

Iranian Journal of Catalysis (IJC)

https://doi.org/10.57647/j.ijc.2024.1403.32

Triethylammonium chloride modified graphene oxide as a novel and the highly efficient catalyst for the production of bis-coumarins

Kosar Daneshpajooh, Esmael Rostami*

Department of Basic Sciences, Faculty of chemistry, Payame Noor University, Tehran, Iran.

***Corresponding author:** e.rostami@pnu.ac.ir ; esmaelrostami@gmail.com

[Original Research

Received:
23 March 2024
Revised:
18 May 2024
Accepted:
8 August 2024
Published online:
31 August 2024

Abstract:

This research reports the synthesis of bis-coumarins using graphene oxide functionalized by triethylammonium chloride (GO@TETA-CAC-Et_3N^+.Cl^-) as a sustainable and efficient catalyst. The synthesis was achieved through the reaction of 4-hydroxycoumarin and benzaldehydes via a multicomponent reaction under no-solvent conditions. Firstly, graphene oxide was produced by a modified Hummers procedure and treated with triethylenetetramine. The product was subsequently modified by chloroacetyl chloride and then triethylamine to achieve the catalyst (GO@TETA-CAC-Et_3N^+.Cl^-). The catalyst structure was then confirmed by FESEM, thermogravimetric analysis (TGA), XRD, EDS, X-ray elemental mapping technique, and FTIR. The catalyst offered some advantages over conventional ones, including environmental compatibility, stability, cost-effectiveness, and nonmetal components, as well as recoverability and safe handling. The applied procedure is superior to other methods due to its easy workup, sustainability, solvent-free medium, high yield, short reaction time, and no byproduct.

Keywords: Graphene oxide; Synthesis; Bis-coumarin; Multicomponent reaction; Green chemistry

1. Introduction

Environmental problems have gained significant attention in recent years, and a large number of studies have focused on overcoming these crises. As a solution, green chemistry principles have been approved to diminish chemical toxicity [1]. Green chemistry involves the design of safe chemical processes to minimize or eliminate the production of hazardous products and the use of toxic reagents and solvents [2]. Heterogeneous and sustainable catalysts are important players in the field of green chemistry to design environmentally benign processes and stable procedures for repetitive reloading under reaction conditions [3]. Compared to homogeneous catalysts, heterogeneous ones offer higher yields and selectivity in organic synthesis, more structural stability and flexibility in preparation and application, and less toxic [4]. Moreover, the use of solvent-free conditions [5] or environmentally friendly solvents and no use of toxic solvents help the ecosystems [6]. Energy consumption management is an important goal of green chemistry to avoid high temperatures and the destruction of ecosystems [7].

The one-step synthesis of organic compounds and complex structures is a challenge in material science for the design of advanced materials with exceptional properties. One approach involves the use of convergent, efficient, and concise reactions [8, 9]. Multicomponent reactions (MCRs) refer to the one-pot synthesis of molecules from three or higher starting materials at high yields [10]. They are efficiently used for the synthesis of heterocycles and small organic molecules. Despite MCRs, multistep reactions use high volumes of toxic solvents and reagents while requiring several isolation and purification steps [11]. Green chemistry uses MCRs to achieve higher yields and less by-products at lower toxic materials to protect the environment [12]. MCRs have modified the synthesis of materials in medicinal chemistry, drug discovery, natural product synthesis, polymer chemistry, agrochemistry, and combinatorial chemistry [13].

Carbon-based catalysts are among the sustainable and eco-

friendly candidates that can be employed for the construction of a series of catalysts [14, 15]. Graphene and graphene oxide are two main backbones that can be modified and functionalized with organic moieties such as amines and sulfonic acids to achieve desirable catalysts [16, 17]. Their catalyst derivatives have been used to prepare various organic compounds [18, 19]. Moreover, a large number of hybrid materials have been designed based on graphene, graphene oxide, polymers, metal-organic frameworks (MOF), natural products, inorganic oxides, metallic and other nanoparticles, and clay minerals to be applied in various fields and disciplines, including chemistry and material science [20, 21].
The coumarin structure bears a connected benzene and pyran ring. Bis-coumarol (dicoumarol) is a coumarin derivative with anticoagulant activity. They are heterocyclic compounds [22] from natural or synthetic origins. These compounds have exhibited various biological features, including enzyme inhibitor, anticoagulant, anti-parasite, antibacterial, and anti-insect activities [23]. Coumarins have exhibited a series of applications in chemistry and material science, including light-sensitive photoinitiators/photosensitizers, smart materials, fluorescent chemosensors, photoredox catalysis, and corrosion inhibitors [24]. The synthesis of bis-coumarins has been well studied using diverse methods with multicomponent and multistep reactions [25]. The one-pot multicomponent reaction of 4-hydroxycoumarin and aldehydes is the main synthetic procedure [26]. The common synthetic route including 4-hydroxycoumarin and aldehydes has been implemented by various catalytic systems such as organic-inorganic hybrid magnetic nanomaterial [27], Fe_3O_4@sulfosalicylic acid MNPs [28], $Fe(SD)_3$ [29], chitosan and functionalized graphene oxide nanocomposite [30], Fe_3O_4@SiO_2-$(CH_2)_3$-Pyridine-2-(1H)-tetrazole-Cu(II) [31], heteropolyacids [32], acetic acid functionalized poly(4-vinylpyridinum) bromide [33], [bmim]BF_4 ionic liquid [34], and nano-[SiO_2@R-Im-SO_3H][CF_3COO] [35]. The reported procedures suffer from several disadvantages that necessitate the development of modified procedures.
In the present work, graphene oxide was modified with triethylenetetramine, chloroacetyl chloride, and triethylamine. After characterization, it was employed as an efficient catalyst to prepare bis-coumarins in a sustainable medium.

2. Experimental

2.1 Materials and instrumentation

Reagents and materials were synthetic and analytical grades and acquired from Fluka and Merck and used as received. A Thermal Scientific apparatus was utilized to obtain melting points, and Thermogravimetric analysis (TGA) was conducted on an SDT Q600 V20.9 Build 20 apparatus. Scanning electron microscope (A Tescan Mira III, Czech) equipped with energy-dispersive X-ray spectroscopy (EDS or EDAX) was also employed to study the morphology through field emission scanning electron microscopy (FESEM), and elemental analyses (EDS and MAP). The samples were explored using FTIR spectroscopy (BRUKER spectrometer) and X-ray diffraction (XRD) (PW1730 diffractometer).

2.2 Synthesis of graphene oxide

Graphene oxide was prepared via the modified Hummers methods [36]. At first, a 1000 mL round-bottomed flask was charged with 90 mL of sulfuric acid and cooled in an ice bath, followed by adding 2.0 g sodium nitrate and 2.0 g graphite. The flask content was stirred. After 4h, potassium permanganate was slowly added in two portions (2×3 g). Then, the ice bath was removed after 40 min. and the mixture was stirred at room temperature for 48h. Afterward, 180 mL of deionized water was slowly added while the temperature was rapidly raised to 90 °C. After stirring and cooling down to room temperature, 200 mL of deionized water was charged, followed by adding hydrogen peroxide (8 mL). The color of the reaction mixture turned yellow after complete oxidation in the presence of hydrogen peroxide. The mixture was stirred for 4h, and then hydrochloric acid (concentrated, 8 mL) was charged. After 30 min., stirring was stopped, and the graphite oxide precipitate was purified using a centrifuge, and the precipitate was suspended in 100 mL of deionized water and sonicated for 30 min. The new precipitate was purified via centrifugation and washed using deionized water and, ethanol, and then acetone. Ultimately, the precipitate was left at room temperature to achieve dried graphene oxide.

2.3 Production of triethylenetetramine-functionalized graphene oxide (GO@TETA)

Graphene oxide (1.0 g) was suspended in dimethylacetamide (DMAc, 30 mL) and ultrasonicated for 30 min. at room temperature. Then, triethylenetetramine (0.40 mL), triethylamine (0.70 mL), and DCC (3 mmol, 0.6 g) were added. The reaction was continued at room temperature for 48h, and the mixture was diluted with 4 mL of water and 30 mL dimethylsulfoxide, warmed, and collected via filtration. Ultimately, the purified product was afforded via treatment with hot ethanol, double distilled water, and then acetone. The product was then left at room temperature to attain fine black powders.

2.4 Preparation of graphene oxide functionalized with triethylenetetramine and chloroacetyl chloride (GO@TETA-CAC)

In a typical procedure, GO@TETA (1.0 g) was suspended in 30 mL of dimethylacetamide and converted to a colloidal solution via sonication at room temperature. Then, 0.60 mL chloroacetyl chloride and 0.90 mL triethylamine were added and stirred at room temperature for 48h. Ultimately, the mixture was diluted with 4 mL of deionized water and 30 mL of dimethylsulfoxide, warmed, and filtered. The precipitate on filter paper was treated with hot ethanol, followed by deionized water and then acetone. The resulting precipitate was left at room temperature to attain a fine black powder as GO@TETA-CAC.

2.5 Preparation of graphene oxide functionalized with triethylenetetramine, chloroacetyl chloride, and triethylamine (GO@TETA-CAC-Et_3N^+.Cl^-)

The mixture of graphene oxide functionalized with triethylenetetramine and chloroacetyl chloride (GO@TETA-

CAC) (1.0 g) and dried acetonitrile (30 mL) was prepared and treated in an ultrasonic bath for 30 min. at room temperature. Then, 1.0 mL of triethylamine was charged into the resulting colloidal solution, and the mixture was heated at 80 °C for 24h. Ultimately, the pure product was obtained via centrifugation and treated with ethyl acetate and acetone. The precipitate was heated in an oven at 50 °C, and the final product was afforded.

2.6 General procedure for the synthesis of bis-coumarins using the catalyst

The homogenized mixture of 4-Hydroxycoumarin (2 mmol, 0.32 g) and aldehyde (1 mmol) was treated with a catalyst (0.02 g) and heated using an oil bath for the appropriate time. The completion of the reaction was determined using TLC, and then 5 mL of ethyl acetate was added and filtered hot. The precipitate on the filter paper was washed with hot ethyl acetate several times and dried as a recovered catalyst, and the mother liquor was distilled to attain a crude precipitate. The purified bis-coumarin product was achieved using alcohol as a crystallization solvent. The recoverability and reusability of the catalyst were studied for **3d** for five times.

^{1}H NMR spectrum of 3c

^{1}H NMR (300 MHz, DMSO-d$_6$) δ : 6.29 (s, 1H), 6.67 (d, J= 9Hz, 2H), 6.98 (d, J= 6 Hz, 2H), 7.34 – 7.48 (m, 5H), 7.60 – 7.66 (m, 3H), 7.94 (dd, J= 3, 6 Hz, 3H) ppm.

^{1}H NMR spectrum of 3k

^{1}H NMR (300 MHz, DMSO-d$_6$) δ : 6.13 (s, 1H), 7.26 – 7.54 (m, 7H), 7.57 (dd, J= 3, 6 Hz, 2H), 7.86 – 7.91 9 (m, 2H), 12.57 (b, 2H) ppm

3. Results and Discussion

3.1 Synthesis and characterization of catalyst

The modified Hummers method was utilized for the production of graphene oxide using strong oxidation agents such as concentrated sulfuric acid, $NaNO_3$, hydrogen peroxide, and $KMnO_4$ [36]. Ultrasonication in deionized water is a key step in the preparation of single-layer nanostructured graphene oxide. Graphene oxide was treated with triethylenetetramine using triethylamine and DCC to afford GO@TETA product (Scheme 1). Then, GO@TETA was treated with chloroacetyl chloride to afford the acetyl chloride functionalized graphene oxide (GO@TETA-CAC). Finally, GO@TETA-CAC was treated with triethylamine to afford the catalyst (GO@TETA-CAC-$Et_3N^+.Cl^-$) (Scheme 2).

FTIR spectrum of graphene oxide (Fig. 1a) shows wavenumbers higher than 3000 cm^{-1} as stretching vibrations of hydroxyls [37]. Vibrations at 2959 and 2825 cm^{-1} indicated the presence of aliphatic CH functional groups [38]. Carbonyl of ketones can be determined at 1722 cm^{-1} [39], while carbonyl and CH groups were detected at 1623 cm^{-1} [40]. The presence of ether groups can be confirmed by the emergence of a peak at 1177 cm^{-1} [41].

The FTIR spectrum of GO@TETA (Fig. 1b) showed the stretching vibrations of hydroxyls, NH amines, and NH amides at 3441 cm^{-1} [42]. Meanwhile, the peaks at 2854 and 2924 cm^{-1} can be assigned to aliphatic CH functional groups [38]. Also, frequencies of carboxylic acid carbonyls can be determined at 1725 cm^{-1} [43], whereas the vibrations of amide carbonyls, C=C, and C=N functional can be observed at 1647 cm^{-1} [44].

Moreover, vibrations at 1575 cm^{-1} can be attributed to the

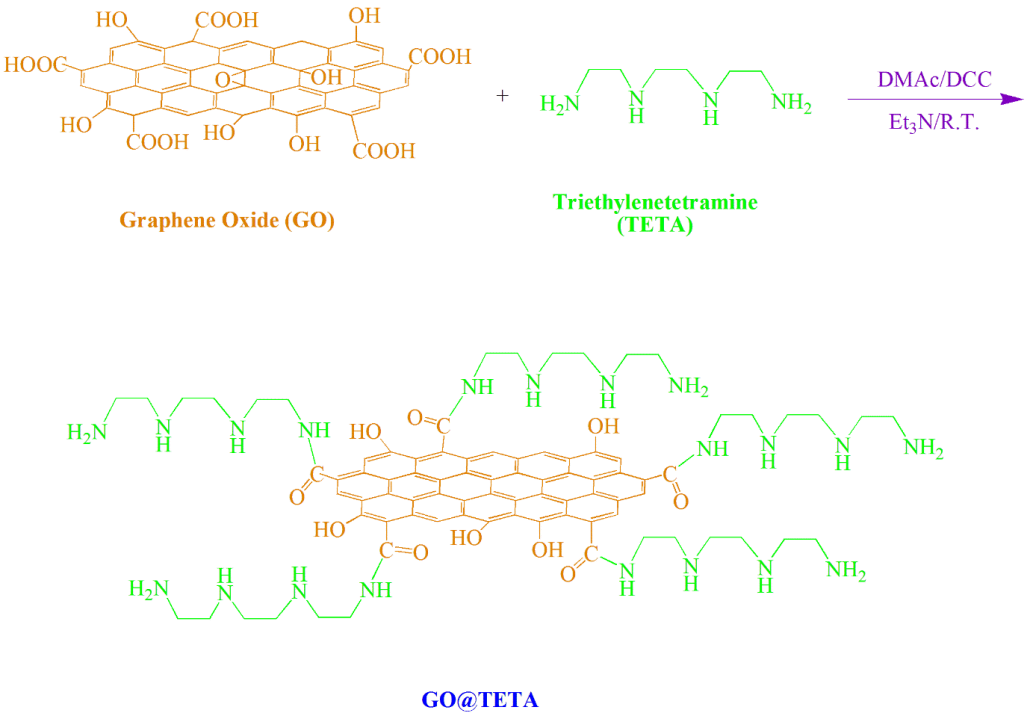

Scheme 1. Preparation of GO@TETA.

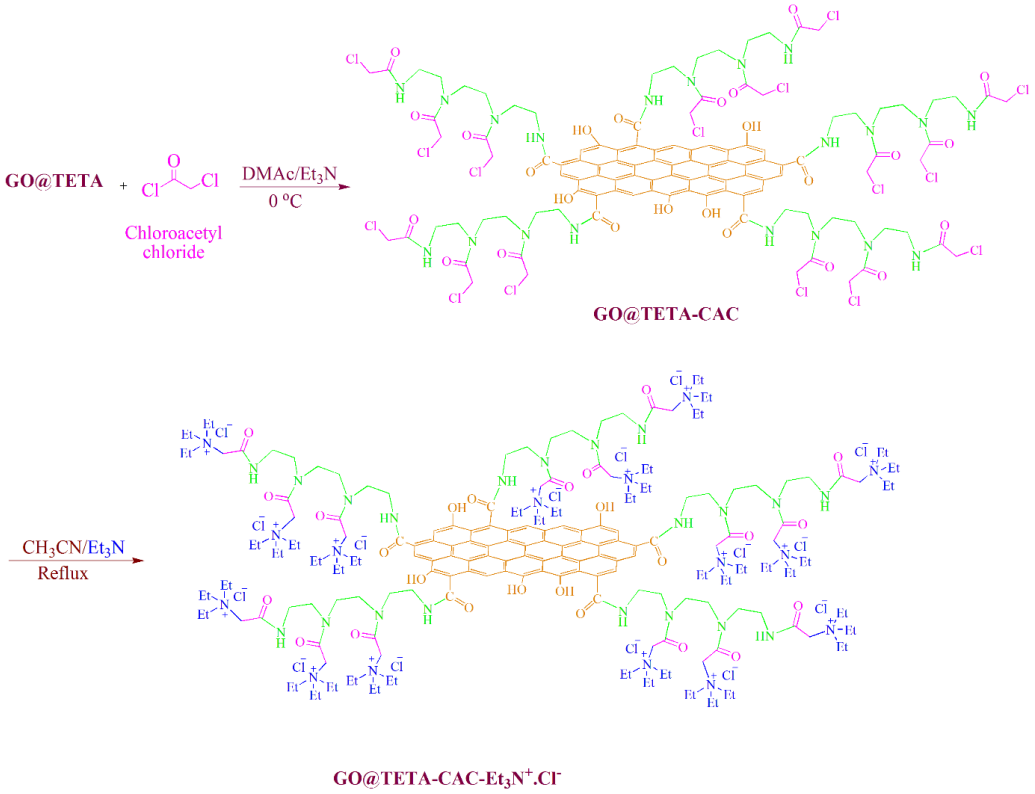

Scheme 2. Preparation of catalyst (GO@TETA-CAC- $Et_3N^+.Cl^-$).

C=C moiety of benzene rings and carboxylates [45]. The band at 1439 cm^{-1} shows CH and carboxylate groups [46]. Further, the peak at 1387 cm^{-1} indicates the presence of C=O (COO), C-N, and bending modes of CH functional [47]. Frequencies of C-O-C epoxy structure were detected at 1243 cm^{-1} [48]. Additionally, frequencies belonging to C-N bonds can be observed at 1076 cm^{-1} [49], while the peak at 1026 cm^{-1} exhibits the etheric C-O moiety [50]. Furthermore, C-N vibrations can be detected at 617 cm^{-1} [51].

Fig. 2a shows the FTIR spectrum of graphene oxide functionalized with triethylenetetramine and chloroacetyl chloride (GO@TETA-CAC) where the vibrational frequencies at 3437 cm^{-1} exhibited stretching vibrations of O-H, NH amines, and amides [42]. The peaks at 2922 and 2853 cm^{-1} imply the vibrations of aliphatic CH functional groups [38]. Vibrations at 1722 cm^{-1} can be assigned to the carbonyl of ketone [43] while the vibrations of carbonyl (C=O), C=C, and C-N groups can be detected at 1629 cm^{-1} [52]. The peaks at 1565 cm^{-1} belong to

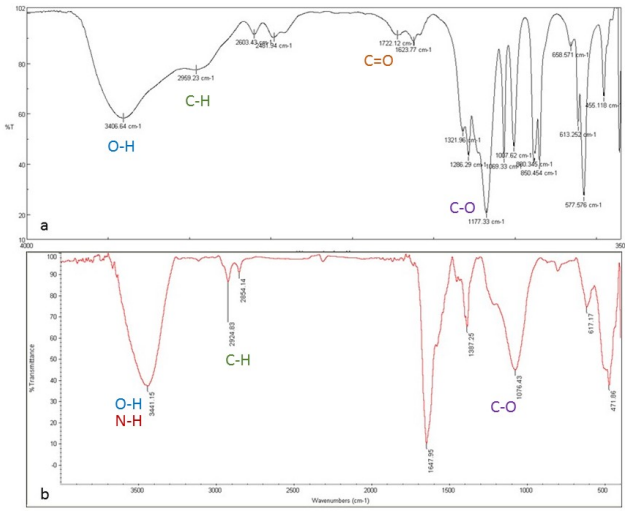

Figure 1. FTIR spectra of (a) graphene oxide and (b) GO@TETA.

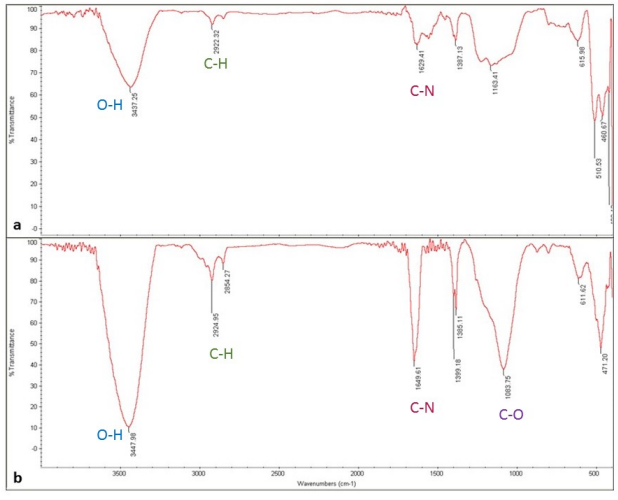

Figure 2. FTIR spectra of (a) GO@TETA-CAC and (b) catalyst (GO@TETA-CAC-$Et_3N^+.Cl^-$).

stretching vibrations of C=C groups of benzene rings [53]. The peak at 1387 cm^{-1} can be assigned to the carbonyl of carboxylate, C-N, and aliphatic CH moieties [47]. Vibrations of C-O-C and C-OH functional groups can be observed at 1215 cm^{-1} [54]. The peaks at 1163 and 1000 cm^{-1} can also be ascribed to CH and etheric functional groups [55]. Vibrations of C-Cl functional can be detected at 615 cm^{-1} [56], C-N vibrations can be observed at 510 cm^{-1} [57], and vibrations of plane ring deformations can be detected at 460 cm^{-1} [58].

Vibrations of hydroxyls, NH amine, and NH amide of catalyst can be detected at 3447 cm^{-1} (Fig. 2b) [42]. Frequencies of 2924 and 2854 cm^{-1} are associated with aliphatic CH_2 and CH_3 functional groups [38]. Whereas the peak at 1725 cm^{-1} corresponds to carbonyl groups [43]. The peak appearing at 1649 cm^{-1} is also related to the carbonyl of amide functional groups [52]. Vibrations at 1575 cm^{-1} can be attributed to C=C and carboxylate of graphene oxide [47, 53], whereas the vibrations at 1399 cm^{-1} are associated with the CH_2 and C-N functional [47]. Vibrations of CH_2 and C-O-H functional groups can be observed at 1385 cm^{-1} [47]. The peak at 1220 cm^{-1} is related to etheric C-O-C [59], while the peak at 1083 cm^{-1} determines the C-O-C moieties. Moreover, the band at 1000-1200 cm^{-1} corresponds to the etheric C-O group [60]. The presence of CH_3 functional can be confirmed based on the peak emerging at 617 cm^{-1} [61]. The vibrations of C-O groups resulted in a peak at 471 cm^{-1} [62]. Based on the FTIR spectra of graphene oxide functionalized with triethylenetetramine, chloroacetyl chloride, and triethylamine, the structure of the catalyst was improved.

Fig. 3 shows the XRD spectra of GO, GO@TETA, GO@TETA-CAC, and catalyst (GO@TETA-CAC-$Et_3N^+.Cl^-$). The peak at 2θ=11 ° demonstrates the graphene oxide structure [63], while a broad and weak peak at 2θ=18-22 ° confirms the presence of reduced graphene oxide (Fig. 3a). Spectrum of GO@TETA can be found in Fig. 3b which revealed a sharp peak at 2θ=12 ° and a broad one 2θ=18-28 ° belonging to graphene oxide and nanostructured reduced graphene oxide, respectively [64]. Another small peak at 42 ° suggests the crystalline structure of graphite. XRD pattern of GO@TETA-CAC showed a peak at 2θ=13 ° and non-crystalline nanostructured material shows a broad peak at 2θ=18-28 °, and a sharp peak at 27 ° demonstrates a sample with various interlayer distances (Fig. 3c).

Fig. 3d shows the XRD pattern of the catalyst, which demonstrates a peak at 2θ=11 ° due to GO. Non-crystalline reduced graphene oxide moiety resulted in a peak at 2θ=18-30 ° [65]. Also, a peak at 42 ° demonstrates the crystalline graphite. XRD patterns of graphene oxide, GO@TETA, GO@TETA-CAC, and catalyst show an increase in the synthesis of the non-crystalline and nanostructured nature of graphene oxide. Also, peak positions and d-spacing of samples are reported in Table 1.

The FESEM images of GO@TETA, GO@TETA-CAC and catalyst can be found in Fig. 4 which reveals the nanostructured particles with conglomerate structure. Polar groups on the sheets and edges of graphene oxide increased the particle size and conglomerate nature of structures [66]. Fig. 5 shows the EDS analysis of GO@TETA and GO@TETA-CAC. Accordingly, GO@TETA contains carbon, nitrogen, and oxygen (Fig. 5a), confirming the functionalization of graphene oxide with triethylenetetramine. Moreover, GO@TETA-CAC encompasses carbon, nitrogen, oxygen, and chlorine (Fig. 5b), confirming the functionalization of graphene oxide with triethylenetetramine and chloroacetyl chloride. Additionally, Fig. 6 shows the EDS analysis of the catalyst, which confirms the presence of carbon, nitrogen, oxygen, and chlorine on the surface, implying the modification of graphene oxide with triethylenetetramine and chloroacetyl chloride and then triethylamine.

The X-ray mapping analysis of the catalyst revealed the

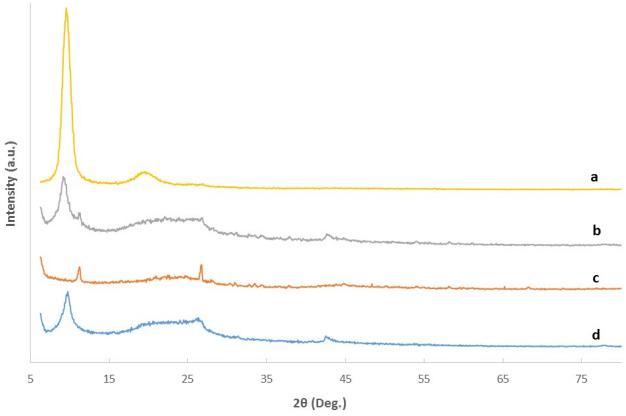

Figure 3. XRD patterns of (a) GO, (b) GO@TETA, (c) GO@TETA-CAC, and (d) catalyst.)

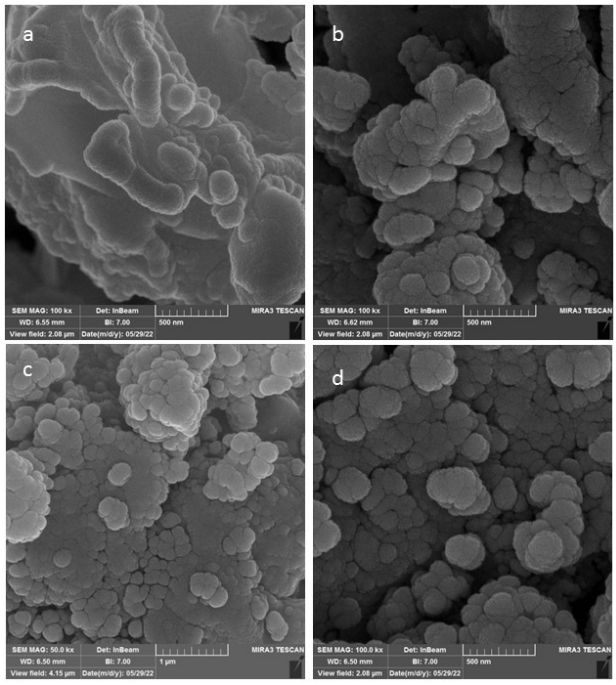

Figure 4. FESEM images of (a) GO@TETA, (b) GO@TETA-CAC, and (c,d) GO@TETA-CAC-$Et_3N^+.Cl^-$.

Table 1. Peak positions and d-spacing of samples in XRD studies

GO		GO@TETA	
2θ (°)	**d** (*Å*)	**2θ** (°)	**d** (*Å*)
9.62	9.18	9.22	9.58
		26.71	3.33
		42.75	2.11
GO@TETA-CAC		**GO@TETA-CAC-Et_3N^+.Cl^-**	
2θ (°)	**d** (*Å*)	**2θ** (°)	**d** (*Å*)
11.22	7.88	9.72	9.09
26.69	3.33	26.43	3.37
		42.53	2.12

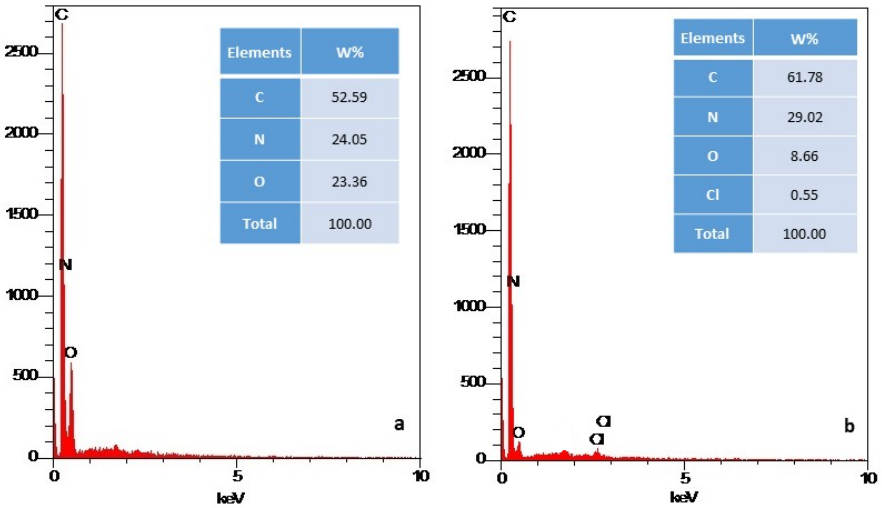

Figure 5. EDS analysis of (a) GO@TETA, (b) GO@TETA-CAC.

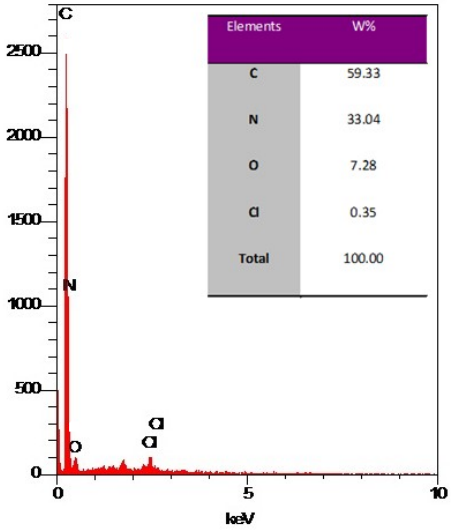

Figure 6. EDS analysis of catalyst.

elemental distribution of carbon, nitrogen, oxygen, and chloride in separate images and in a combined image (Fig. 7). Furthermore, the surface morphology of the sample was reported using an SEM image.

The thermal stability of catalysts under reaction conditions was explored by thermogravimetric analysis (TGA). To this end, the sample was heated under an argon atmosphere from 30 to 500 °C (Fig. 8). Three weight losses can be determined. The first one at around 100 °C is due to the evaporation of solvents and adsorbed small molecules [67].Weight loss between 150 to 200 °C is probably the consequence of the desorption of physisorbed large

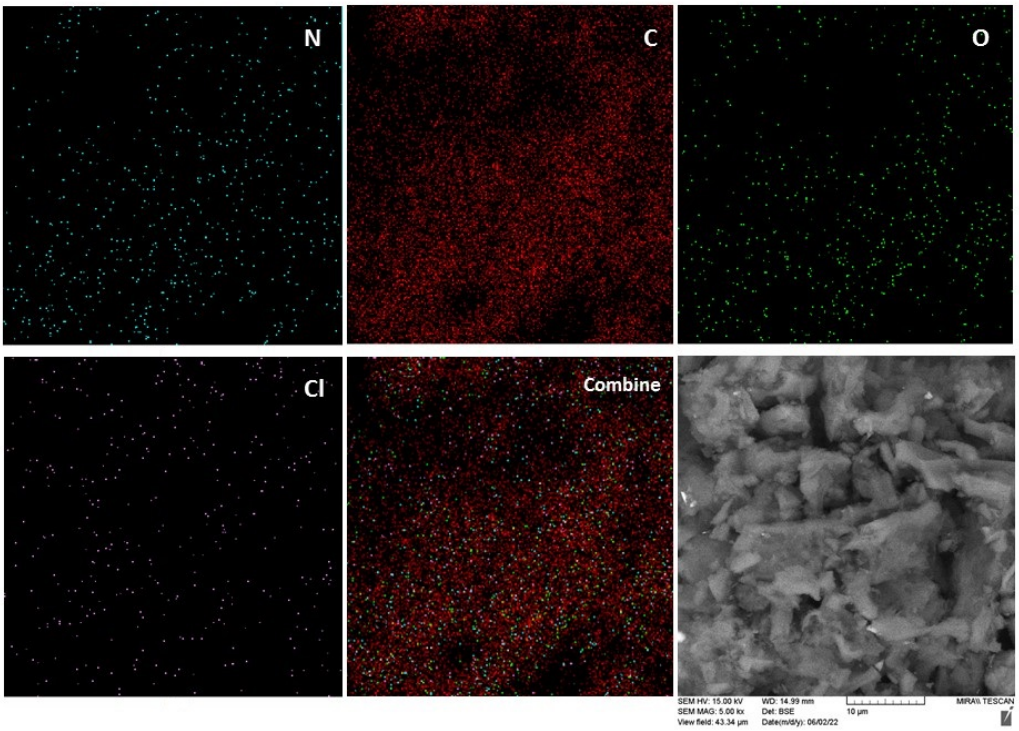

Figure 7. X-ray mapping analysis and SEM image of the catalyst.

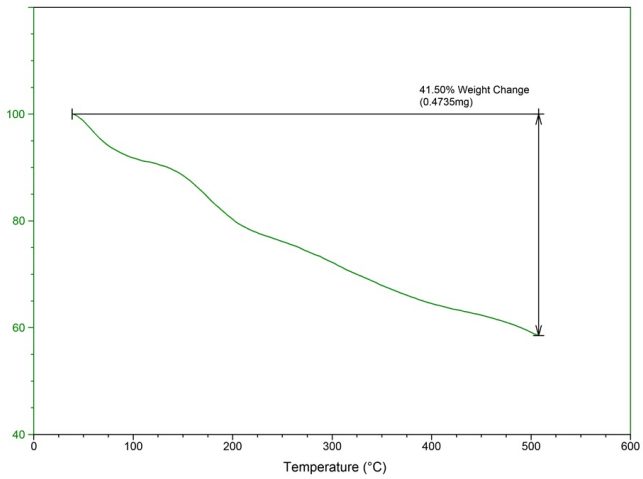

Figure 8. Thermogravimetric analysis (TGA) of catalyst.

molecules [68]. Separation of functional groups and destruction of graphene oxide structure occurred at 310 °C and 420 °C. Addressing the diagram, total weight change and char yield were 41.50% and 58.50%, suggesting the stability of the catalyst. Thus, the catalyst can be employed up to 200 °C, making it a significant candidate for the study of sustainable carbon materials.

3.2 Synthesis of bis-coumarins

The developed catalyst is carbon-based with some advantages, which can be used for the preparation of bis-coumarins using 4-hydroxycoumarin and aryl aldehydes. To optimize the reaction conditions, the synthesis of **3d** was studied considering a series of variables (Scheme 3, Table 2). 4-Hydroxycoumarin, aryl aldehyde, and catalyst were mixed and heated in an oil bath, and TLC was applied to investigate the reaction progress. TLC studies were performed using n-hexane/ethyl acetate (4:1) and one drop of acetic acid. Finally, the mixture was diluted with ethyl acetate and filtered hot. The catalyst was collected on filter paper, and the mother liquor was distilled; the precipitate was recrystallized in ethanol to achieve **3d** as pure bis-coumarin. The precipitate on filter paper was washed several times with dry ethyl acetate and chloroform. The recovered catalyst can be used for the reaction again for several times (Fig. 9).

The synthesis of **3d** was explored at optimized conditions (Table 2, Entry 4), which includes no solvent, catalyst (0.02 g), and temperature of 90 °C for 20 min, with 95% yield. To determine the functional group scope of the reaction, a

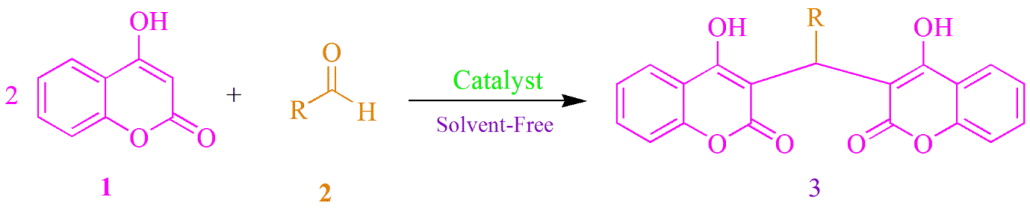

Scheme 3. Production of bis-coumarins using GO@TETA-CAC-Et_3N^+.Cl^- catalyst.

Table 2. Optimum conditions using GO@TETA-CAC-Et_3N^+.Cl^- catalyst for the synthesis of **3d**.

Entry	Solvent	Catalyst (g)	Temperature (°C)	Time (min)	Yield (%)[1]
1	Solvent-free	0.01	100	30	69
2	Solvent-free	0.01	110	30	75
3	Solvent-free	0.02	100	20	96
4	Solvent-free	0.02	90	20	95
5	Solvent-free	0.02	80	20	88
6	Solvent-free	0.02	70	25	82
7	Solvent-free	0.03	90	20	95
8	Solvent-free	0.04	90	20	96
9	Solvent-free	0.03[2]	90	40	35
10	Solvent-free	0.03[3]	90	40	63
11	Ethanol	0.02	Reflux	90	74
12	Methanol	0.02	Reflux	90	58
13	DMF	0.02	90	90	61
14	CH_3CN	0.02	Reflux	90	47
15	H_2O	0.02	Reflux	90	65
16	Toluene	0.02	Reflux	90	63

[1]Isolated yield, [2]GO, [3]GO@TETA

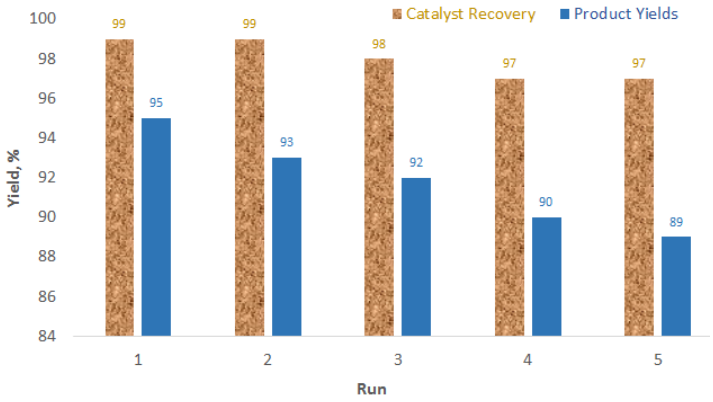

Figure 9. Catalyst recovery and reuse for preparation of **3d** in five cycles.

series of aldehydes were employed as reported in Table 3. Higher product yields were afforded with electron accepting functional and halogen on aldehydes while aldehydes with electron releasing functional led to lower yields [86]. To confirm the structure of the products, their melting points were compared with previous reports, and ^{1}H NMR confirmed the structures of **3c** and **3k**.

3.3 Reaction mechanism

Scheme 4 shows a plausible mechanism for the reaction of 4-hydroxycoumarin and aldehydes using the catalyst. The catalyst was activated aldehyde via ammonium moiety [87] and activated 4-hydroxycoumarin via chloride ion. Also, 4-hydroxycoumarin attacked the aldehyde and afforded intermediate **II**. Then, **III** was afforded by water elimination from **II** using the catalyst through ammonium salt activation [88]. In the next step, another activated coumarin molecules attached **III** through a 1,4-addition (Michael addition) to achieve **IV** and a keto-enol tautomerization [89] achieved the final bis-coumarin product.

3.4 Catalyst recovery and reuse

Synthesis of **3d** was selected as a model reaction to study the recovery and reusability of the catalyst as representative

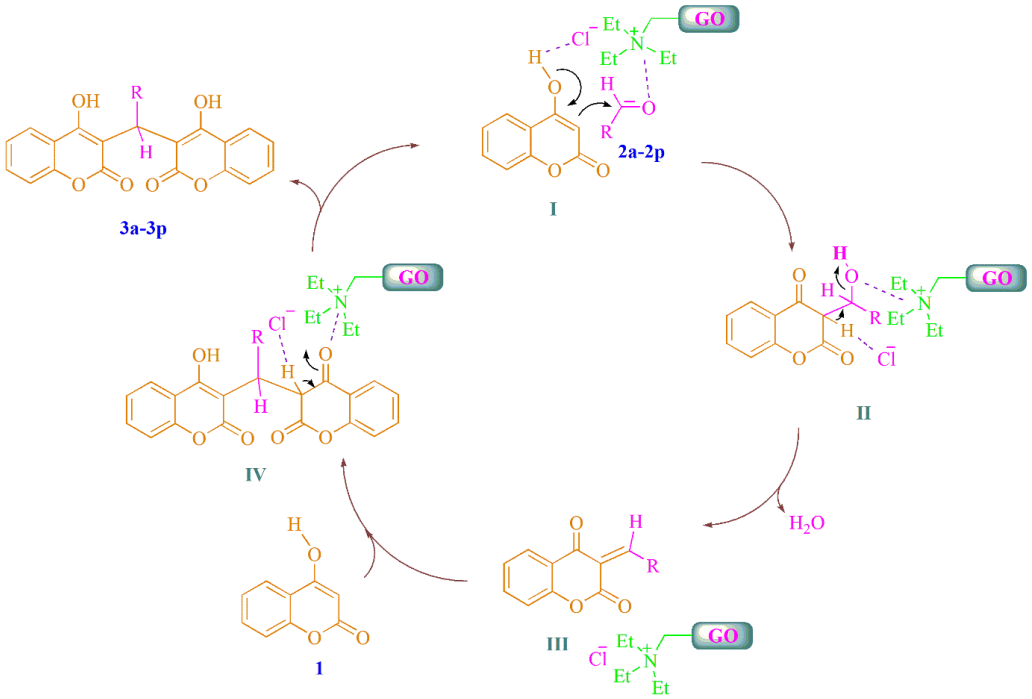

Scheme 4. Plausible mechanism for the synthesis of bis-coumarin.

Table 3. Synthesis of bis-coumarin products utilized GO@TETA-CAC-Et_3N^+.Cl^- catalyst

Entry	R	Product	Time (min)	Yield (%)[1]	MP (°C)	
					Measured	Reported [Ref.]
1	4-ClC_6H_4	**3a**	20	96	258 – 259	258 – 260 [69]
2	3,4-$(OMe)_2$ C_6H_3	**3b**	35	90	263 – 264	262 – 264 [70]
3	4-OHC_6H_4	**3c**	20	94	222 – 223	220 – 223 [71]
4	3-$NO_2C_6H_4$	**3d**	20	95	239 – 240	240 – 242 [72]
5	4-N,N-dimethylC_6H_4	**3e**	30	92	220 – 221	222 – 224 [69]
6	4-$NO_2C_6H_4$	**3f**	30	94	239 – 240	238 – 240 [69]
7	4-$OMeC_6H_4$	**3g**	35	89	254 – 255	254 – 256 [71]
8	2-ClC_6H_4	**3h**	20	93	203 – 204	200 – 202 [73]
9	4-MeC_6H_4	**3i**	30	90	264 – 265	265 – 267 [72]
10	C_6H_5	**3j**	25	93	233 – 234	233 – 234 [69]
11	2,4-diClC_6H_3	**3k**	25	90	201 – 202	200 – 202 [73]
12	2-OHC_6H_4	**3l**	30	87	256 – 257	256 – 258 [74]
13	4-BrC_6H_4	**3m**	20	95	253 – 254	255 – 257 [72]
14	4-Pyridyl	**3n**	30	95	275 – 277	276 – 277 [75]
15	2-Furanyl	**3o**	30	92	202 – 204	201 – 202 [76]
16	CH_3CH_2	**3p**	30	86	240 – 242	239 – 240 [77]

[1]Isolated yields

variables for exploring durability, stability, and activity in the synthesis and reaction conditions. The synthesis of **3d** was repeated five times, and through each run, the recovered catalyst was purified using ethyl acetate and chloroform to be reused in the next step (Fig. 9). The findings are reported in Fig. 9, which reveal no significant change in the catalyst recovery yields and **3d** yields. Thus, under reaction conditions, the structure of the catalyst undergoes minimum changes, and the functional groups responsible for the catalytic activity remained stable.

3.5 Comparison with other catalysts

The efficiency of the GO@TETA-CAC-Et_3N^+.Cl^- catalyst was compared with other reported catalysts. According to Table 4, solvent-free condition, catalyst loading, product yield, and reaction time were evaluated and compared with other catalysts during the synthesis of **3d**. Moreover, the toxicity and sustainability of the catalyst were evaluated

Table 4. Comparison of the catalyst with other reported ones for the synthesis of **3d**

Entry	Catalyst	Amounts of Catalyst	Solvent	Time (Min)	Temperature (°C)	Yield (%) [Ref.]
1	GO@TETA-CAC-$Et_3N^+.Cl^-$	0.02 g	Solvent-free	20	90	95 [-]
2	Humic Acid	0.01g	Solvent-free	15	100	97 [78]
3	CSC@Pt	0.05g	Ethanol	7	Reflux	97 [79]
4	P_4VPy	0.02g	H_2O	10	90	92 [80]
5	Fe_3O_4@SiO_2@Ni–Zn–Fe LDH	0.02g	H_2O	10	Reflux	95 [73]
6	HNPs@Py	0.01g	Solvent-free	22	RT	90 [72]
7	$[Et_3NH][HSO_4]$	0.04g	Solvent-free	5	110	85 [81]
8	Fe_3O_4@$B(HSO_4)_3$	0.03w%	Solvent-free	20	80	85 [82]
9	D-ribose based ionic liquid	5mol%	Ethanol	90	80	81 [83]
10	Fe_3O_4@SMF@THSB	0.03w%	Solvent-free	10	80	73 [84]
11	Fe_3O_4@SiO_2@KCC-1@MPTMS@Cu^{II}	0.01g	Solvent-free	25	70	94 [85]

based on the applied metals or structure of the catalyst. The reported catalysts mainly contain toxic metals or very toxic organic moieties or non-recoverable with difficult separation. Thus, the developed catalyst was superior over other catalysts and can be efficiently applied in organic synthesis and material science.

4. Conclusions

Graphene oxide was functionalized with triethylenetetramine and chloroacetyl chloride and then triethylaminum chloride and used as a productive catalyst for bis-coumarin synthesis. The synthesis proceeded under solvent-free conditions in the sustainable medium. For the preparation of the catalyst, graphene oxide was first modified with triethylenetetramine and treated with chloroacetyl chloride and then with triethylamine. The synthesis was conducted at high yields through the pseudo-three component one-pot reaction of 4-hydroxycoumarin and aldehydes using the catalyst. The conditions were expanded for other aldehydes with various functional groups. The electron-accepting groups and halogens offered higher yields compared to electron-donating ones. The catalyst and conditions have priorities, for instance, no use of solvent, sustainability, carbon-based catalyst, and nonmetal, inexpensive, and stable under reaction conditions. Compared to other catalysts, the developed catalyst offers some advantages, including being carbon-based and nonmetal, sustainable with nontoxic or less toxic organic moieties, recoverability, stability under reaction conditions, cost-effectiveness, the use of medium reaction conditions, and easy transfer and storage. Regarding the mentioned properties, this catalyst is a promising candidate for further studies in chemistry and related disciplines.

Acknowledgement
We are grateful to the Payame Noor University, Tehran Research Council, for the support of this research.

Authors Contributions
Authors were equally contributed in acquisition and analysing the data as well as preparing the paper.

Availability of Data and Materials
Data is available on request from the corresponding author, upon reasonable request.

Conflict of Interests
The authors declare that they have no known competing financial interests or personal relationships that could have appeared to influence the work reported in this paper.

References

[1] P. Anastas and N. Eghbali. Green chemistry: principles and practice. *Chem. Soc. Rev*, **39**(2010):301–12. DOI: https://doi.org/10.1039/B918763B.

[2] J. B. Zimmerman, P. T. Anastas, H. C. Erythropel, and W. Leitner. Designing for a green chemistry future. *Science*, **367**(2020):397–400. DOI: https://doi.org/10.1126/science.aay3060.

[3] H. Mousavi. A comprehensive survey upon diverse and prolific applications of chitosan-based catalytic systems in one-pot multi-component synthesis of heterocyclic rings. *Int. J. Biol. Macromol*, **186**(2021):1003–1166. DOI: https://doi.org/10.1016/j.ijbiomac.2021.06.123.

[4] H. C. Erythropel, J. B. Zimmerman, T. M. de Winter, L. Petitjean, F. Melnikov, C. H. Lam, A. W. Lounsbury, K. E. Mellor, N. Z. Janković, Q. Tu, and L. N. Pincus. The green chemistree: 20 years after taking root with the 12 principles. *Green Chem*, **20**(2018):1929–1961. DOI: https://doi.org/10.1039/C8GC00482J.

[5] M. A. Martins, C. P. Frizzo, D. N. Moreira, L. Buriol, and P. Machado. Solvent-free heterocyclic synthesis. *Chem. Rev.*, **109**(2009):4140–4182. DOI: https://doi.org/10.1021/cr9001098.

[6] I. Huskić, C. B. Lennox, and T. Friščić. Accelerated ageing reactions: towards simpler, solvent-free, low energy chemistry. *Green Chem*, **22**(2020):5881–5901. DOI: https://doi.org/10.1039/D0GC02264K.

[7] N. Dey, A. Mandal, R. Jana, A. Bera, S. A. Azad, S. Giri, M. Ikbal, and S. Samanta. 2023 recent development of solvent-free synthesis of heterocycles. *New J. Chem*, **47**(2023):13035–13079. DOI: https://doi.org/10.1039/D3NJ01991H.

[8] A. Domling, W. Wang, and K. Wang. Chemistry and biology of multicomponent reactions. *Chem. Rev.*, **112**(2012):3083–3135. DOI: https://doi.org/10.1021/cr100233r.

[9] R. K. Singh, S. Sharma, A. Sandhar, M. Saini, and S. Kumar. Current development in multicomponent catalytic synthesis of 1, 5-benzodiazepines: a systematic review. *Iran. J. Catal*, **6**(2016):1–21.

[10] B. H. Rotstein, S. Zaretsky, V. Rai, and A. K. Yudin. Small heterocycles in multicomponent reactions. *Chem. Rev.*, **114**(2014):8323–8359. DOI: https://doi.org/10.1021/cr400615v.

[11] S. M. Saied, M. Y. Saleh, and A. M. Hamdoon. Multicomponent synthesis of tetrahydrobenzo [a] xanthene and tetrahydrobenzo [a] acridine derivatives using sulfonated multi-walled carbon nanotubes as heterogeneous nanocatalysts. *Iran. J. Catal*, **12**(2022):189–205. DOI: https://doi.org/10.30495/IJC.2022.1955651.1924.

[12] H. Mousavi, M. Rimaz, and B. Zeynizadeh. Practical three-component regioselective synthesis of drug-like 3-aryl (or heteroaryl)-5, 6-dihydrobenzo [h] cinnolines as potential non-covalent multi-targeting inhibitors to combat neurodegenerative diseases. *ACS Chem. Neurosci*, **15**(2024):1828–1881. DOI: https://doi.org/10.1021/acschemneuro.4c00055.

[13] E. Jahangard, L. Khazdooz, and A. Zarei. Synthesis and in vitro antibacterial study of dihydropyrano [3, 2-c] chromene derivatives by nano fluoro apatite doped with mg and si as a cooperative catalyst. *Iran. J. Catal*, **10**(2020):57–63. URL https://oiccpress.com/iranian-journal-of-catalysis.

[14] E. Rostami and S. Hamidi Zare. Double brønsted acidic media immobilized on carbonized sugarcane bagasse (cscb) as a new and efficient solid acid catalyst for the synthesis of coumarins, dicoumarols and xanthenes. *ChemistrySelect*, **4**(2019):13295–303. DOI: https://doi.org/10.1002/slct.201902864.

[15] N. Saravana Ganesan and P. Suresh. Synthesis of β-amino ketones using graphene oxide: a benign carbonaceous acid catalyst for mannich reaction. *Res. Chem. Intermed.*, **47**(2021):1197–1210, . DOI: https://doi.org/10.1007/s11164-020-04324-3.

[16] E. Rostami and S. M. Haghayeghi. Trifluoroacetate-bonded polyethylene graphene oxide composite as a novel and efficient catalyst for the synthesis of benzimidazoles under solvent-free conditions. *Iran. J. Catal.*, **11**(2021):37–48. URL https://oiccpress.com/iranian-journal-of-catalysis.

[17] N. Saravana Ganesan and P. Suresh. Nitrogen-doped graphene oxide as a sustainable carbonaceous catalyst for greener synthesis: benign and solvent-free synthesis of pyranopyrazoles. *ChemistrySelect*, **5**(2020):4988–4993, . DOI: https://doi.org/10.1002/slct.202000748.

[18] O. Mohammadi, M. Golestanzadeh, and M. Abdouss. Recent advances in organic reactions catalyzed by graphene oxide and sulfonated graphene as heterogeneous nanocatalysts: a review. *New J. Chem.*, **41**(2017):11471–97. DOI: https://doi.org/10.1039/C7NJ02515G.

[19] M. Karthik and P. Suresh. Brønsted acidic reduced graphene oxide as a sustainable carbocatalyst: a selective method for the synthesis of c-2-substituted benzimidazole. *New J. Chem.*, **42**(2018):17931–17938. DOI: https://doi.org/10.1039/C8NJ03257B.

[20] W. Yu, L. Sisi, Y. Haiyan, and L. Jie. Progress in the functional modification of graphene/graphene oxide: a review. *RSC Adv.*, **10**(2020):15328–45. DOI: https://doi.org/10.1039/D0RA01068E.

[21] X. Fan, G. Zhang, and F. Zhang. Multiple roles of graphene in heterogeneous catalysis. *Chem. Soc. Rev.*, **44**(2015):3023–3035. DOI: https://doi.org/10.1039/C5CS00094G.

[22] A. Bouhaoui, M. Eddahmi, M. Dib, M. Khouili, A. Aires, M. Catto, and L. Bouissane. Synthesis and biological properties of coumarin derivatives. a review. *ChemistrySelect*, **6**(2021):5848–70. DOI: https://doi.org/10.1002/slct.202101346.

[23] F. Annunziata, C. Pinna, S. Dallavalle, L. Tamborini, and A. Pinto. An overview of coumarin as a versatile and readily accessible scaffold with broad-ranging biological activities. *Int. J. Mol. Sci.*, **21**(2020):4618. DOI: https://doi.org/10.3390/ijms21134618.

[24] M. Sarmah, K. Chutia, D. Dutta, and P. Gogoi. Overview of coumarin-fused-coumarins: synthesis, photophysical properties and their applications. *Org. Biomol. Chem.*, **20**(2022):55–72. DOI: https://doi.org/10.1039/D1OB01876K.

[25] E. C. Gaudino, S. Tagliapietra, K. Martina, G. Palmisano, and G. Cravotto. Recent advances and perspectives in the synthesis of bioactive coumarins. *RSC Adv*, **6**(2016):46394–405. URL 10.1039/C6RA07071J.

[26] S. Gulati, R. Singh, and S. Sangwan. A review on convenient synthesis of substituted coumarins using reuseable solid acid catalysts. *RSC Adv*, **11**(2021):29130–155. DOI: https://doi.org/10.1039/D1RA04887B.

[27] M. Barzegar, A. Zare, A. Ghobadpoor, and M. Dianat. Preparation, characterization and application of a novel organic-inorganic hybrid magnetic nanomaterial as a highly efficient catalyst for the synthesis of bis-coumarins. *Iran. J. Catal.*, **12**(2022):13–24. DOI: https://doi.org/10.30495/ijc.2022.688895.

[28] Z. Zare-Akbari, S. Dastmalchi, L. Edjlali, L. Dinparast, and M. Es'haghi. A novel nanomagnetic solid acid catalyst for the synthesis of new functionalized bis-coumarin derivatives under microwave irradiations in green conditions. *Appl. Organomet. Chem.*, **34**(2020):e5649. DOI: https://doi.org/10.1002/aoc.5649.

[29] N. O. Mahmoodi, Z. Jalalifard, and G. P. Fathanbari. Green synthesis of bis-coumarin derivatives using fe(sd)$_3$ as a catalyst and investigation of their biological activities. *J. Chin. Chem. Soc.*, **67**(2020):172–82. DOI: https://doi.org/10.1002/jccs.201800444.

[30] Z. Atashrouz, E. Rostami, and A. Zare. Chitosan and functionalized graphene oxide nanocomposite as a novel and highly efficient catalyst for production of bis-coumarins under solvent-free conditions. *Res. Chem. Intermed.*, **48**(2022):179–201. DOI: https://doi.org/10.1007/s11164-021-04616-2.

[31] A. Oji Moghanlou, M. Pourshahi, S. Atabak, and N. Mohammadian Tarighi. The use of recyclable magnetic nanocatalyst fe$_3$o$_4$@ sio$_2$-(ch$_2$)$_3$-pyridine-2-(1h)-tetrazole-cu (ii) in the synthesis of bis-coumarin derivatives under green conditions. *Iran. J. Catal.*, **13**(2023):187–199. DOI: https://doi.org/10.30495/ijc.2023.1982870.2000.

[32] D. Shahzad, A. Saeed, M. Faisal, F. A. Larik, S. Bilquees, and P. A. Channar. Recent synthetic approaches to 3, 3′-(methylene) bis (coumarins). *Org. Prep. Proced. Int.*, **51**(2019):199–239. DOI: https://doi.org/10.1080/00304948.2019.1599788.

[33] E. Noroozizadeh, A. R. Moosavi-Zare, M. A. Zolfigol, M. Zarei, R. Karamian, M. Asadbegy, S. Yari, and S. H. M. Farida. Synthesis of bis-coumarins over acetic acid functionalized poly (4-vinylpyridinum) bromide (apvpb) as a green and efficient catalyst under solvent-free conditions and their biological activity. *J. Iran. Chem. Soc.*, **15**(2018):471–81, . DOI: https://doi.org/10.1007/s13738-017-1247-1.

[34] J. M. Khurana and S. Kumar. Ionic liquid: an efficient and recyclable medium for the synthesis of octahydroquinazolinone and biscoumarin derivatives. *Monatsh. Chem.*, **141**(2010):561–4. DOI: https://doi.org/10.1007/s00706-010-0306-4.

[35] J. Atashrooz and A. Zare. Nano-[sio$_2$@ r-imso$_3$h][cf$_3$coo]: an effectual catalyst for the production of bis-coumarins and n, n′-alkylidene bisamides. *Iran. J. Catal.*, **12**(2022):127–137. DOI: https://doi.org/10.30495/IJC.2022.68983.

[36] R. Muzyka, M. Kwoka, L. Smedowski, N. Diez, and G. Gryglewicz. Oxidation of graphite by different modified hummers methods. *New Carbon Mater*, **32**(2017):15–20. DOI: https://doi.org/10.1016/S1872-5805(17)60102-1.

[37] Y. C. Cao, C. Xu, X. Wu, X. Wang, L. Xing, and K. Scott. A poly (ethylene oxide)/graphene oxide electrolyte membrane for low temperature polymer fuel cells. *J. Power Sources*, **196**(2011):8377–82. DOI: https://doi.org/10.1016/j.jpowsour.2011.06.074.

[38] G. Huang, Z. Ni, G. Chen, G. Li, and Y. Zhao. Investigation of irradiated graphene oxide/ultra-high-molecular-weight polyethylene nanocomposites by esr and ftir spectroscopy. *Fuller. Nanotub. Carbon Nanostructures*, **24**(2016):698–704. DOI: https://doi.org/10.1080/1536383X.2016.1229310.

[39] L. Wei, X. Chen, K. Hong, Z. Yuan, L. Wang, H. Wang, Z. Qiao, X. Wang, Z. Li, and Z. Wang. Enhancement in mechanical properties of epoxy nanocomposites by styrene-ethylene-butadiene-styrene grafted graphene oxide. *Compos. Interfaces*, **26**(2019):141–156. DOI: https://doi.org/10.1080/09276440.2018.1481303.

[40] F. Yuan, H. Z. Chen, H. Y. Yang, H. Y. Li, and M. Wang. Pan–peo solid polymer electrolytes with high ionic conductivity. *Mater. Chem. Phys.*, **89**(2005):390–94. DOI: https://doi.org/10.1016/j.matchemphys.2004.09.032.

[41] Z. Zhang, T. Su, Y. Han, Z. Yang, J. Wei, L. Jin, and H. Fan. A convergent synthetic platform for dual anticancer drugs functionalized by reduced graphene nanocomposite delivery for hepatocellular cancer. *Drug Deliv*, **28**(2021):1982–94. DOI: https://doi.org/10.1080/10717544.2021.1974606.

[42] J. S. Lee, J. C. Yoon, and J. H. Jang. A route towards superhydrophobic graphene surfaces: surface-treated reduced graphene oxide spheres. *J. Mater. Chem. A*, **1**(2013):7312–15. DOI: https://doi.org/10.1039/C3TA11434A.

[43] L. Shao, X. Chang, Y. Zhang, Y. Huang, Y. Yao, and Z. Guo. Graphene oxide cross-linked chitosan nanocomposite membrane. *Appl. Surf. Sci.*, **280**(2013):989–92. DOI: https://doi.org/10.1016/j.apsusc.2013.04.112.

[44] A. A. Yakout, R. H. El-Sokkary, M. A. Shreadah, and O. G. A. Hamid. Cross-linked graphene oxide sheets via modified extracted cellulose with high metal adsorption. *Carbohydr. Polym*, **172**(2017):20–27. DOI: https://doi.org/10.1016/j.carbpol.2017.05.004.

[45] F. Samadaei, M. Salami-Kalajahi, and H. Roghani-Mamaqani. Grafting of poly (acrylic acid) onto poly (amidoamine)-functionalized graphene oxide via surface-mediated reversible addition-fragmentation chain transfer polymerization. *Int. J. Polym. Mater.*, **65**(2016):302–329. DOI: https://doi.org/10.1080/00914037.2015.1119686.

[46] A. Schönemann and H. G. Edwards. Raman and ftir microspectroscopic study of the alteration of chinese tung oil and related drying oils during ageing. *Anal. Bioanal. Chem.*, **400**(2011):1173–80. DOI: https://doi.org/10.1007/s00216-011-4855-0.

[47] M. Portaccio, C. Menale, N. Diano, C. Serri, D. G. Mita, and M. Lepore. Monitoring production process of cisplatin-loaded plga nanoparticles by ft-ir microspectroscopy and univariate data analysis. *J. Appl. Polym. Sci.*, **132**(2015):41305–15. DOI: https://doi.org/10.1002/app.41305.

[48] X. Zhao, H. Zhu, J. Chen, and Q. Ao. Ftir, xrd and sem analysis of ginger powders with different size. *J. Food Process. Preserv.*, **39**(2015):2017–26. DOI: https://doi.org/10.1111/jfpp.12442.

[49] G. Richner and G. Puxty. Assessing the chemical speciation during co_2 absorption by aqueous amines using in-situ ftir. *Ind. Eng. Chem. Res.*, **51**(2012): 14317–24. DOI: https://doi.org/10.1021/ie302056f.

[50] M. M. Paradkar, S. Sakhamuri, and J. Irudayaraj. Comparison of ftir, ft-raman, and nir spectroscopy in a maple syrup adulteration study. *J. Food Sci.*, **67**(2002): 2009–2015. DOI: https://doi.org/10.1111/j.1365-2621.2002.tb09493.x.

[51] B. J. Kim and K. S. Kang. Stopband attenuation of silica spheres by attaching aniline and polyaniline. *Synth. Met.*, **169**(2013):55–58. DOI: https://doi.org/10.1016/j.synthmet.2013.03.007.

[52] V. Dhanabalan, K. M. Xavier, S. Eppen, A. Joy, A. Balange, K. K. Asha, L. N. Murthy, and B. B. Nayak. Characterization of chitin extracted from enzymatically deproteinized acetes shell residue with varying degree of hydrolysis. *Carbohydr. Polym*, **253**(2021):117203. DOI: https://doi.org/10.1016/j.carbpol.2020.117203.

[53] V. Kumar, R. K. Gupta, R. K. Gundampati, D. K. Singh, S. Mohan, S. H. Hasan, and M. Malviya. Enhanced electron transfer mediated detection of hydrogen peroxide using a silver nanoparticle–reduced graphene oxide–polyaniline fabricated electrochemical sensor. *RSC Adv.*, **8**(2018):619–31. DOI: https://doi.org/10.1039/C7RA11466D.

[54] R. K. Cheedarala and J. I. Song. In situ generated hydrophobic micro ripples via π–π stacked pop-up reduced graphene oxide nanoflakes for extended critical heat flux and thermal conductivities. *RSC Adv.*, **9**(2019):31735–46. DOI: https://doi.org/10.1039/C9RA04563E.

[55] C. Pan, H. Gu, and L. Dong. Synthesis and electrochemical performance of polyaniline@ mno_2/graphene ternary composites for electrochemical supercapacitors. *J. Power Sources*, **303**(2016):175–81. DOI: https://doi.org/10.1016/j.jpowsour.2015.11.002.

[56] H. J. Amezquita-Garcia, E. Razo-Flores, F. J. Cervantes, and J. R. Rangel-Mendez. Anchorage of anthraquinone molecules onto activated carbon fibers to enhance the reduction of 4-nitrophenol. *J. Chem. Technol. Biotechnol.*, **90**(2015):1685–1691. DOI: https://doi.org/10.1002/jctb.4478.

[57] C. Pal. Band envelope study of vapor phase ftir spectra of acetamide aided by dft. *J. Mol. Struct.*, **920**(2009):327–31. DOI: https://doi.org/10.1016/j.molstruc.2008.11.022.

[58] W. Li, X. Z. Tang, H. B. Zhang, Z. G. Jiang, Z. Z. Yu, X. S. Du, and Y. W. Mai. Simultaneous surface functionalization and reduction of graphene oxide with octadecylamine for electrically conductive polystyrene composites. *Carbon*, **49**(2011):4724–30. DOI: https://doi.org/10.1016/j.carbon.2011.06.077.

[59] H. Liu, L. Zhang, Y. Guo, C. Cheng, L. Yang, L. Jiang, G. Yu, W. Hu, Y. Liu, and D. Zhu. Reduction of graphene oxide to highly conductive graphene by lawesson's reagent and its electrical applications. *J. Mater. Chem. C*, **1**(2013):3104–9. DOI: https://doi.org/10.1039/C3TC00067B.

[60] R. Hadi, H. Abbasi, E. Payami, I. Ahadzadeh, and R. Teimuri-Mofrad. Synthesis, characterization and electrochemical properties of 4-azidobutylferrocene-grafted reduced graphene oxide-polyaniline nanocomposite for supercapacitor applications. *ChemistrySelect*, **5**(2020):575–83. DOI: https://doi.org/10.1002/slct.201903726.

[61] K. S. Finnie, V. Luca, P. D. Moran, J. R. Bartlett, and J. L. Woolfrey. Vibrational spectroscopy and exafs study of ti ($oc_2h_5)_4$ and alcohol exchange in ti (iso-$oc_3h_7)_4$. *J. Mater. Chem.*, **10**(2000):409–18. DOI: https://doi.org/10.1039/A906662D.

[62] W. J. Meng, X. Y. Han, Y. L. Hou, Y. Xie, J. Zhang, C. J. He, and D. L. Zhao. Defect-repaired reduced graphene oxide caging silicon nanoparticles for lithium-ion anodes with enhanced reversible capacity and cyclic performance. *Electrochim. Acta*, **382**(2021):138271. DOI: https://doi.org/10.1016/j.electacta.2021.138271.

[63] F. T. Johra, J. W. Lee, and W. G. Jung. Facile and safe graphene preparation on solution based platform. *J. Ind. Eng. Chem.*, **20**(2014):2883–87. DOI: https://doi.org/10.1016/j.jiec.2013.11.022.

[64] T. H. Thi Vu, T. T. Thi Tran, H. N. Thi Le, P. H. Thi Nguyen, N. Q. Bui, and N. Essayem. A new green approach for the reduction of graphene oxide nanosheets using caffeine. *Bull. Mater. Sci.*, **38**(2015):667–71. DOI: https://doi.org/10.1007/s12034-015-0896-x.

[65] H. Mahdavi, P. K. Kahriz, H. Gholipour-Ranjbar, and T. Shahalizade. Synthesis and performance study of amino functionalized graphene aerogel grafted with polyaniline nanofibers as an efficient supercapacitor material. *J. Mater. Sci. Mater. Electron.*, **28**(2017): 4295–305. DOI: https://doi.org/10.1007/s10854-016-6053-5.

[66] T. J. Fraga, M. N. Carvalho, M. G. Ghislandi, and M. A. D. Motta. Functionalized graphene-based materials as innovative adsorbents of organic pollutants: a concise overview. *Braz. J. Chem. Eng.*, **36**(2019):1–31. DOI: https://doi.org/10.1590/0104-6632.20190361s20180283.

[67] A. Jeyaseelan, N. Viswanathan, M. Naushad, and C. Bathula. Fabrication of multi-functionalized graphene oxide doped alginate hybrid spheres for enhanced fluoride adsorption. *J. Inorg. Organomet. Polym. Mater.*, **32**(2022):216–28. DOI: https://doi.org/10.1007/s10904-021-02163-2.

[68] N. L. Far, E. Rostami, and G. R. Bardajee. Production, characterization, and application of a novel chitosan-g-maleic anhydride and modified graphene oxide nanocomposite, supported methane sulfonic acid, for efficient synthesis of 1-(benzothiazolylamino) methyl-2-naphtols. *Res. Chem. Intermed.*, **47**(2021): 4721–43. DOI: https://doi.org/10.1007/s11164-021-04538-z.

[69] Z. Benzekri, S. Sibous, A. Ouasri, S. Boukhris, A. Hassikou, A. Rhandour, and A. Souizi. Bis [hydrazinium (1^+)] hexafluoridosilicate:(n_2h_5) $2sif_6$ novel hybrid crystal as an efficient, reusable and environmentally friendly heterogeneous catalyst for knoevenagel condensation and synthesis of biscoumarin derivatives. *J. Mol. Struct.*, **1230**(2021):129890. DOI: https://doi.org/10.1016/j.molstruc.2021.129890.

[70] S. K. Patil, D. V. Awale, M. M. Vadiyar, S. A. Patil, S. C. Bhise, and S. S. Kolekar. Simple protic ionic liquid $[et_3nh][hso_4]$ as a proficient catalyst for facile synthesis of biscoumarins. *Res. Chem. Intermed.*, **43**(2017):5365–76. DOI: https://doi.org/10.1007/s11164-017-2932-5.

[71] I. A. Rather and R. Ali. An efficient and versatile deep eutectic solvent-mediated green method for the synthesis of functionalized coumarins. *ACS Omega*, **7**(2022):10649–59. DOI: https://doi.org/10.1021/acsomega.2c00293.

[72] F. Afsharnadery, K. Khosravi, and M. A. Zolfigol. A novel magnetically recyclable semi-dendrimer catalyst-based ethanolpyridole supported on ferrite nanoparticles (hnps@ py) for the synthesis of biscoumarin and dihydropyrano [3, 2-c] chromene derivatives. *Appl. Organomet. Chem.*, **35**(2021):e6297. DOI: https://doi.org/10.1002/aoc.6297.

[73] B. Zeynizadeh M. Gilanizadeh. Synthesis of acridinediones and biscoumarins using fe_3o_4@ sio_2@ ni–zn–fe ldh as an efficient magnetically recoverable mesoporous catalyst. *Polycycl. Aromat. Compd.*, **41**(2021):15–32. DOI: https://doi.org/10.1080/10406638.2019.1567560.

[74] A. E. Hallaoui, S. Chehab, T. Ghailane, B. Malek, O. Zimou, S. Boukhriss, A. Souizi, and R. Ghailane. Application of phosphate fertilizer modified by zinc as a reusable efficient heterogeneous catalyst for the synthesis of biscoumarins and dihydropyrano [3, 2-c] chromene-3-carbonitriles under green conditions. *Polycycl. Aromat. Compd.*, **41**(2021):2083–2102. DOI: https://doi.org/10.1080/10406638.2019.1710853.

[75] E. Noroozizadeh, A. R. Moosavi-Zare, M. A. Zolfigol, M. Zarei, R. Karamian, M. Asadbegy, S. Yari, and S. H. M. Farida. Synthesis of bis-coumarins over acetic acid functionalized poly (4-vinylpyridinum) bromide (apvpb) as a green and efficient catalyst under solvent-free conditions and their biological activity. *J. Iran. Chem. Soc.*, **15**(2018):471–481, . DOI: https://doi.org/10.1007/s13738-017-1247-1.

[76] J. Soni, N. Sahiba, A. Sethiya, P. Teli, D. K. Agarwal, A. Manhas, P. C. Jha, D. Joshi, and S. Agarwal. Biscoumarin derivatives as potent anti-microbials: graphene oxide catalyzed eco-benign synthesis, biological evaluation and docking studies. *Polycycl. Aromat. Compd.*, **42**(2022):2970–2990. DOI: https://doi.org/10.1080/10406638.2020.1852277.

[77] K. Tabatabaeian, H. Heidari, A. Khorshidi, M. Mamaghani, and N. O. Mahmoodi. Synthesis of biscoumarin derivatives by the reaction of aldehydes and 4-hydroxycoumarin using ruthenium (iii) chloride hydrate as a versatile homogeneous catalyst. *J. Serb. Chem. Soc.*, **77**(2012):407–413. DOI: https://doi.org/10.2298/JSC110427189T.

[78] B. Mitra and P. Ghosh. Humic acid: a biodegradable organocatalyst for solvent-free synthesis of bis (indolyl) methanes, bis (pyrazolyl) methanes, bis-coumarins and bis-lawsones. *ChemistrySelect*, **6**(2021):68–81. DOI: https://doi.org/10.1002/slct.202004245.

[79] M. Jokar, H. Naeimi, and G. Nabi Bidhendi. Design and preparation of platinum anchored on cellulose as heterogeneous nanocatalyst for synthesis of bis-coumarin derivatives. *Polycycl. Aromat. Compd.*, **42**(2022):4994–5005. DOI: https://doi.org/10.1080/10406638.2021.1922468.

[80] L. Nazemi Nasirmahale, O. Goli Jolodar, F. Shirini, and H. Tajik. Poly (4-vinylpyridine) ($p_4$vpy): a basic catalyst for facile synthesis of biscoumarin and dihydropyrano [3, 2-c] chromene derivatives in aqueous media. *Polycycl. Aromat. Compd.*, **41**(2021):199–210. DOI: https://doi.org/10.1080/10406638.2019.1576748.

[81] Z. Karimi-Jaberi, B. Masoudi, A. Rahmani, and K. Alborzi. Triethylammonium hydrogen sulfate [et_3nh][hso_4] as an efficient ionic liquid catalyst for the synthesis of coumarin derivatives. *Polycycl. Aromat. Compd.*, **40**(2017):99–107. DOI: https://doi.org/10.1080/10406638.2017.1363061.

[82] P. Hayati, K. Eghbali, and R. Rezaei. Magnetic nanoparticles tris (hydrogensulfato) boron as an efficient heterogeneous acid catalyst for the synthesis of α, α'-benzylidene bis (4-hydroxycoumarin) derivatives under solvent-free condition. *Res. Chem. Intermed.*, **45**(2019):5067–5089. DOI: https://doi.org/10.1007/s11164-019-03881-6.

[83] P. Garg and S. Rajasekhara Reddy. Organocatalytic approach for biscoumarin synthesis via a biomass-derived sustainable strategy. *ChemistrySelect*, **8**(2023):e202301634. DOI: https://doi.org/10.1002/slct.202301634.

[84] A. R. Tahmasebi Sarvestani, R. Rezaei, A. Ghiasi Moaser, and S. Rouhani. Two inorganic shells based on core–shell magnetic sulfonated melamine formaldehyde as sustainable catalysts for the synthesis of biscoumarins. *React. Kinet. Mech. Catal.*, **136**(2023): 3009–3025. DOI: https://doi.org/10.1007/s11144-023-02497-7.

[85] B. Zeynizadeh and H. Mousavi. Diverse and efficient catalytic applications of new cockscomb flower-like fe_3o_4@sio_2@kcc-1@mptms@cu^{II} mesoporous nanocomposite in the environmentally benign reduction and reductive acetylation of nitroarenes and one-pot synthesis of some coumarin compounds. *RSC Adv.*, **12**(2022):11164–11189. DOI: https://doi.org/10.1039/d1ra08763k.

[86] B. Kharrngi, E. D. Dhar, G. Basumatary, D. Das, R. C. Deka, A. K. Yadav, and G. Bez. Developing a highly potent anthelmintic: study of catalytic application of l-proline derived aminothiourea in rapid synthesis of biscoumarins and their in vitro anthelmintic essay. *J. Chem. Sci.*, **133**(2021):1–15. DOI: https://doi.org/10.1007/s12039-020-01881-3.

[87] S. Tanaka, T. Nakashima, T. Maeda, M. Ratanasak, J. Y. Hasegawa, Y. Kon, M. Tamura, and K. Sato. Quaternary alkyl ammonium salt-catalyzed transformation of glycidol to glycidyl esters by transesterification of methyl esters. *ACS Catal.*, **8**(2018):1097–1103. DOI: https://doi.org/10.1021/acscatal.7b03303.

[88] S. Cai, D. Zhu, Y. Zou, and J. Zhao. Porous polymers bearing functional quaternary ammonium salts as efficient solid catalysts for the fixation of co_2 into cyclic carbonates. *Nanoscale Res. Lett.*, **11**(2016):1–9. DOI: https://doi.org/10.1186/s11671-016-1529-z.

[89] D. Kim, S. Subramanian, D. Thirion, Y. Song, A. Jamal, M. S. Otaibi, and C. T. Yavuz. Quaternary ammonium salt grafted nanoporous covalent organic polymer for atmospheric co_2 fixation and cyclic carbonate formation. *Catal. Today*, **356**(2020):527–534. DOI: https://doi.org/10.1016/j.cattod.2020.03.050.